

Supporting Information

Enhanced conversion reaction kinetics in low crystallinity SnO₂/CNT anodes for Na-ion batteries

Jiang Cui,^{a, b} Zheng-Long Xu,^a Shanshan Yao,^a Jiaqiang Huang,^a Jian-Qiu Huang,^a Sara Abouali,^a Mohammad Akbari Garakani,^a Xiaohui Ning^{*b} and Jang-Kyo Kim^{*a}

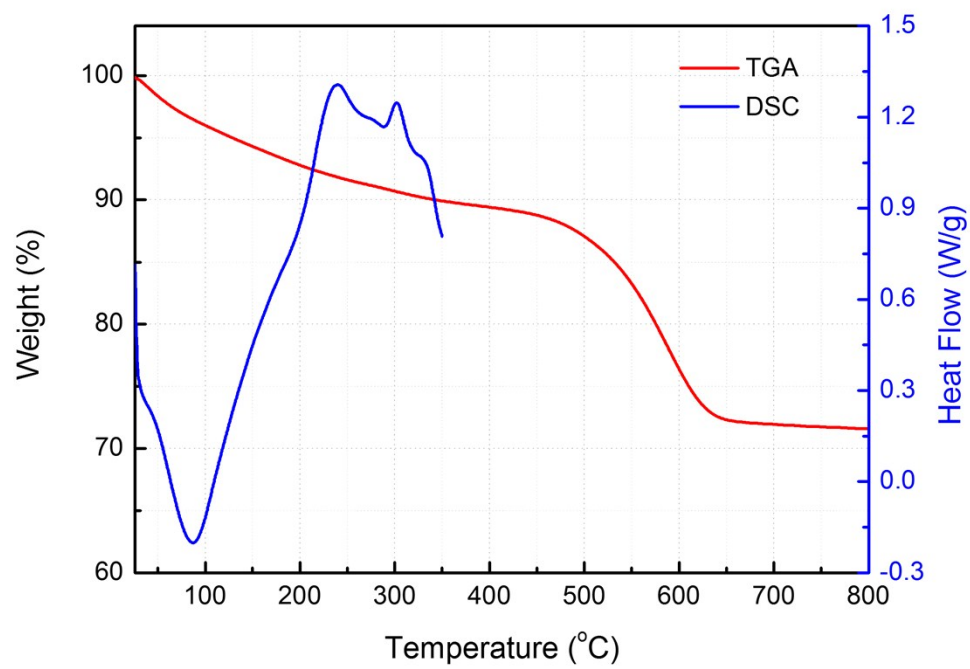


Figure S1 TGA and DSC curves of A-SnO₂/CNT composites.

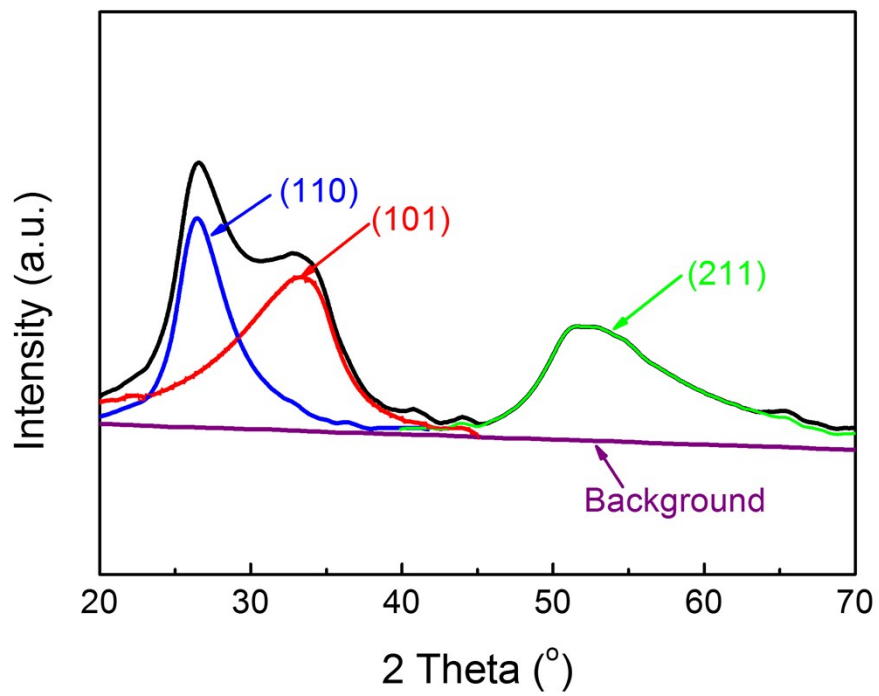


Figure S2 XRD fitting curves of A-SnO₂/CNT composites.

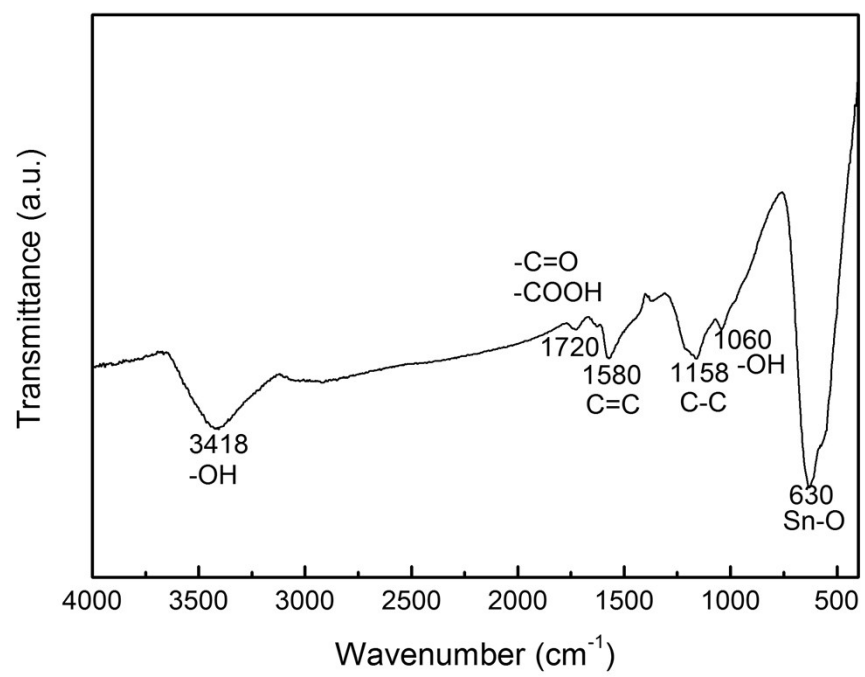


Figure S3 FTIR spectrum of A-SnO₂/CNT electrodes.

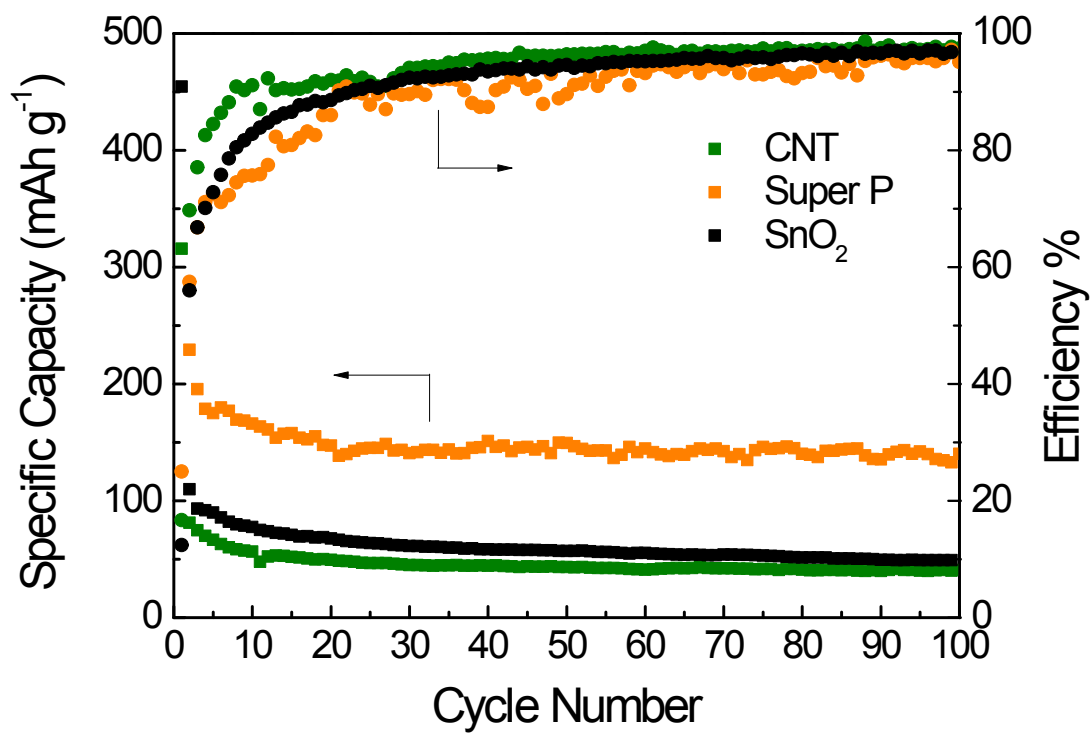


Figure S4 Cyclic performance of pure CNT, Super P and SnO₂ under current density of 0.1 A g⁻¹.

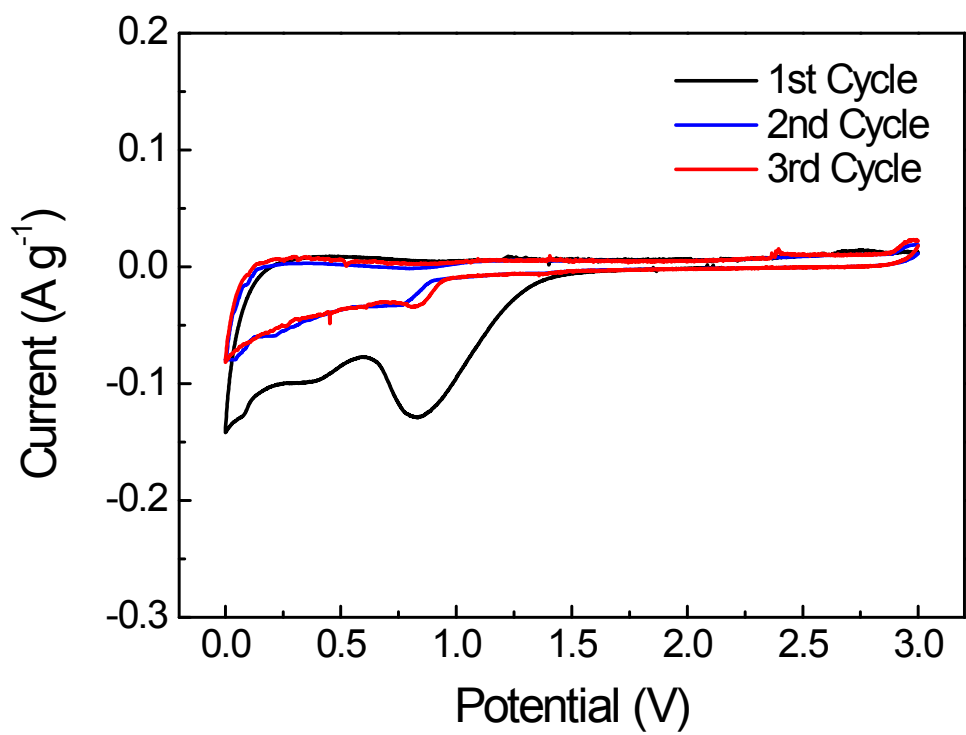


Figure S5 CV curves of pure CNT electrodes at a scan rate of 0.1 mV s⁻¹.

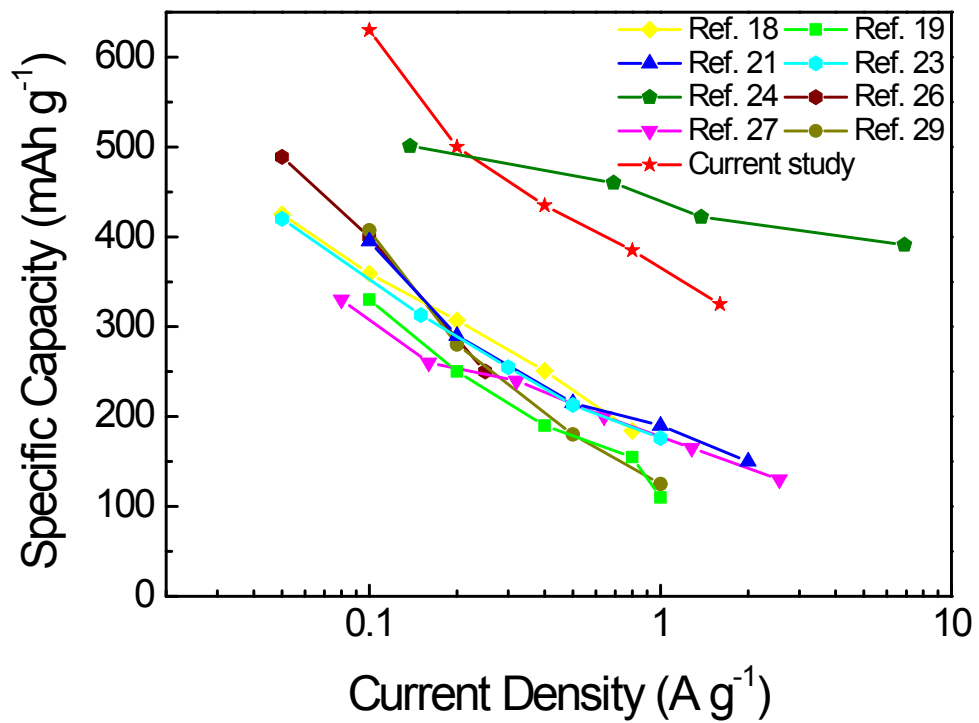


Figure S6 Comparison of specific capacities between the current A-SnO₂/CNT and SnO₂-based anodes taken from the literature.

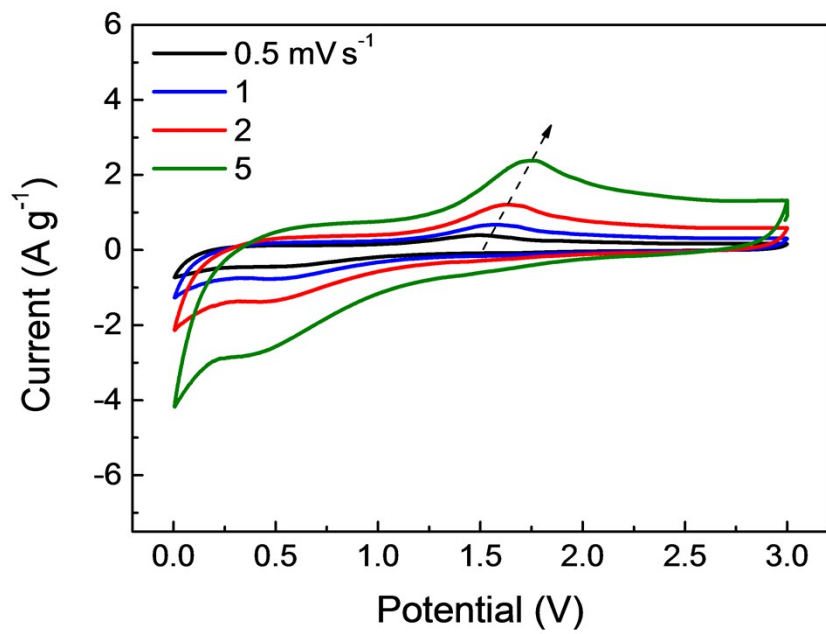


Figure S7 CV curves of C-SnO₂/CNT electrodes at different scan rates.

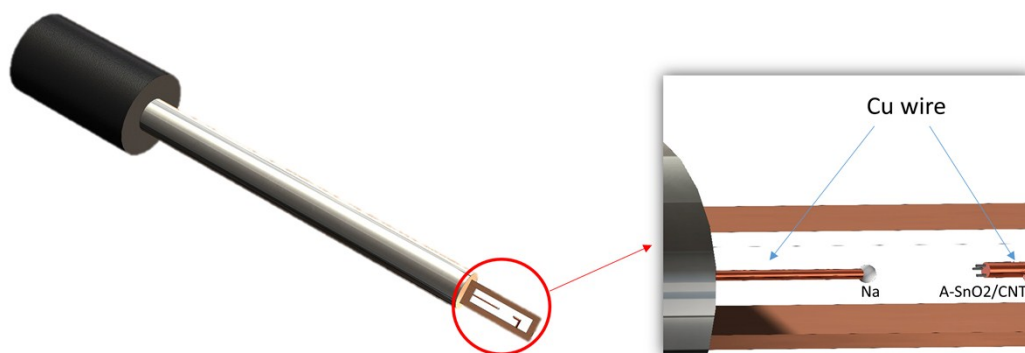


Figure S8 Schematic illustration of *in situ* electrochemical test setup.

Table S1 Comparison of cyclic performance of SnO₂-based anodes in SIBs.

| Materials | Initial reversible capacity | | Cyclic performance | | Ref. |
|-----------------------------|--|--------------------------------------|--|--------------|---------------|
| | Specific capacity (mAh g ⁻¹) | Current density (A g ⁻¹) | Specific capacity (mAh g ⁻¹) | Cycle Number | |
| PCNF/SnO ₂ /C | 452 | 0.05 | 374 | 100 | 18 |
| SnO ₂ /PANI | ~280 | 0.05 | 214 | 400 | 19 |
| SnO ₂ /C | 412 | 0.05 | 239 | 50 | 20 |
| SnO ₂ /G aerogel | 380 | 0.05 | 221 | 200 | 21 |
| SnO ₂ /CNT/C | 452 | 0.05 | 200 | 300 | 23 |
| C/SnO ₂ /CC | 522 | 0.134 | 313 | 100 | 24 |
| SnO ₂ /MWCNT | 489 | 0.05 | 352 | 50 | 26 |
| SnO ₂ /C | 531 | 0.08 | 430 | 200 | 27 |
| SnO ₂ thin film | 300 | 0.1 | 200 | 100 | 28 |
| SnO ₂ /rGO | 407 | 0.1 | 330 | 150 | 29 |
| SnO ₂ /CNT | 630 | 0.1 | 453 | 100 | Current study |
| | 324 | 1.6 | 223 | 300 | study |